Effects of an avidin-biotin binding system on Schwann cells attachment, proliferation, and gene expressions onto electrospun scaffolds

Sha Feng,[1]* Zuoqin Yan,[1] Changan Guo,[1] Zhengrong Chen,[1] Kuihua Zhang,[2] Xiumei Mo,[2] Yudong Gu[3]

[1]Department of Orthopedics, Zhongshan Hospital of Fudan University, 180 Fenglin Road, Shanghai 200032, People's Republic of China
[2]State Key Laboratory for Modification of Fibers, Donghua University, 2999 North Renmin Road, Shanghai 201620, People's Republic of China
[3]Department of Hand Surgery, Huashan Hospital of Fudan University, 12 Middle Wulumuqi Road, Shanghai 200040, People's Republic of China

Received 23 February 2010; revised 6 January 2011; accepted 10 January 2011
Published online 29 March 2011 in Wiley Online Library (wileyonlinelibrary.com). DOI: 10.1002/jbm.a.33063

Abstract: Effective Schwann cells (SCs) attachment is a prerequisite for the successful construction of tissue-engineered nerve. The present study aimed to investigate the role of an avidin-biotin binding system (ABBS) for neural tissue engineering. The attachment, proliferation, and morphology of biotinylated SCs on avidin-treated scaffolds were examined, and the effects of avidin, biotin, and the avidin-biotin binding system on SCs gene expressions were also studied. The results indicated that the attachment of biotinylated SCs onto avidin-treated scaffolds was promoted obviously within a short time (10 min). Meanwhile, there were no great differences in terms of proliferation and morphology of SCs between the two groups after cultivation for 14 days. The gene expressions of S100, GDNF, BDNF, NGF, CNTF, and PMP22 were up-regulated significantly by biotin rather than aligned scaffolds or avidin. The present study demonstrated that ABBS enhanced the attachment and maturation of SCs onto the electrospun scaffolds without adverse effects on the proliferation of SCs in the long term, suggesting the potential application of ABBS in the neural tissue engineering. © 2011 Wiley Periodicals, Inc. J Biomed Mater Res Part A: 97A: 321–329, 2011.

Key Words: ABBS, Schwann cells, cell attachment, maturation

INTRODUCTION

Peripheral nerve defect remains an unsolved clinical challenge due to the limitation of autologous nerve supplies. Tissue-engineered nerve, combining scaffolds and Schwann cells (SCs), is a very promising way to replace the traditional autologous nerve graft.[1–3] An ideal scaffold onto which SCs attach, proliferate, and migrate plays a key role in neural tissue engineering.[4] So far, synthetic degradable polymers have shown outstanding biocompatibility, controllable degradation, high reproducibility, and favorable plasticity.[5] But these synthetic polymers lack adhesion proteins for cells attachment. It has been demonstrated that effective SCs attachment was a prerequisite for the successful construction of tissue-engineered nerve.[6]

Several strategies have been used to promote SCs attaching onto the scaffolds, and the most favored method is to physically absorb or chemically conjugate extracellular matrix (ECM) adhesion proteins to biomaterial surfaces,[7,8] which is based on the formation of integrin-mediated bonds between cell adhesion molecules on substrata and integrin receptors in the cell membrane. But there are two disadvantages of this approach. One is that the efficacy of cells attachment depends on the availability of cell membrane integrin receptors, so this integrin-mediated mechanism may not be beneficial for those cells possessing few integrin receptors. The other is that the ECM from nonhuman species contains exogenous proteins, which may induce immunoreaction and severe fibroplasia in neural tissue, and subsequently hinder the repair of peripheral nerve.[9,10]

Recently, an avidin-biotin binding system (ABBS), a novel integrin-independent binding system, has been applied to tissue engineering. ABBS utilizes a pair of molecules of avidin and biotin, which binds to each other. When used in tissue engineering, biotin is conjugated to the cell membrane, and avidin is immobilized to biomaterial surfaces.[11] The bond formation between these two molecules could mediate cells attaching onto biomaterial surfaces. A major feature of ABBS is its extraordinarily high affinity, which increases the cell adhesion strength. The bond affinity of avidin for biotin is 10^{15} M^{-1}, as compared with that of the integrin receptors for fibronectin

**Present address:* Department of Orthopedics, Zhongshan Hospital Qingpu Branch of Fudan University, 1158 East Gongyuan Road, Shanghai 201700, People's Republic of China.
Correspondence to: Z. Yan; e-mail: yan.zuoqin@zs-hospital.sh.cn or X. Mo; e-mail: xmm@dhu.edu.cn
Contract grant sponsor: Shanghai Natural Science Foundation; contract grant number: 10411962500

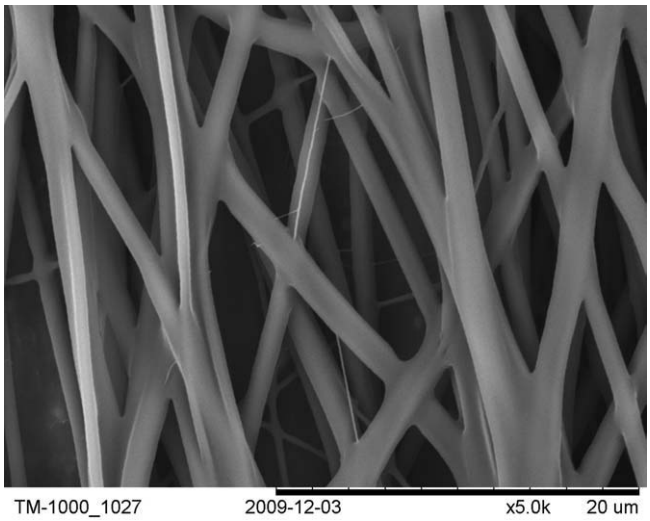

FIGURE 1. The SEM micrograph of P(LLA-CL) (75:25) nanofibers.

which is 10^6 M^{-1}.[12,13] Kuo and Lauffenberger therefore have predicted an increase in the cell adhesion strength by a factor of 2–3 for the avidin-biotin binding system over the integrin-serum protein system.[14] Another feature of ABBS is the fast bonding between avidin and biotin to form a strong noncovalent biochemical bond. Tsai et al. demonstrated that more than 70% biotinylated cells attached onto the avidin-treated substrate, while less than 32% normal cells attached onto the untreated substrate in the first hour.[15] The study of Kojima et al. suggested that ABBS significantly improved initial cell attachment onto biodegradable polymer surfaces in 10 min, while more time was required (over 10 min) to form a stable adhesion complex between integrin and collagen.[16] Bhat et al. reported that the high affinity of the avidin-biotin binding system increased initial cell adhesion, cell spreading rate, and strength of cell attachment.[17] ABBS seems to be a promising way to promote cell attaching onto scaffolds; however, its role in neural tissue engineering has not been reported so far. The present study is to investigate the effects of ABBS on the SCs' attachment, proliferation, and gene expressions.

MATERIALS AND METHODS

Materials

Schwann cells lineage. Schwann cells (SCs) lineage (RSC96) was purchased from ATCC (USA). The cells were cultivated in a mixture of Dulbecco's modified Eagle's cell growth medium: nutrient mixture F-12 (DMEM-F12, 1:1; Gibco, USA) containing 10% fetal bovine serum (Hyclone, Israel) and penicillin/streptomycin (100 U/ml; Gibco, USA), in a humidified environment at 37°C/5% CO_2 on poly-*L*-lysine coated tissue culture flasks. The cell culture medium was changed every day.

Preparation of scaffolds. We chose synthetic degradable copolymer of poly(*L*-lactic acid-*co*-ε-caprolactone) (molar ratio: 75:25), which has been proved favorable for tissue engineering.[18] By the technology of electrospinning, the synthetic copolymer was prepared into linear nanofibers, which could be received in order and made into 2D membranes. Aligned P(LLA-CL) (75:25) nanofiber scaffolds was prepared by the State Key Laboratory for Modification of Fibers, Donghua University (Shanghai, China). The P(LLA-CL) (75:25) copolymer was dissolved with acetone in a water bath at 45°C. Polymer concentration of the solution was 8 wt %. For the process of electrospinning, the polymer solution was placed in a 20-mL plastic syringe fitted with a needle with a tip diameter of 0.8 mm. P(LLA-CL) (75:25) nanofibers were fabricated by electrospinning process at applied voltage 15 kV using a high-voltage power supply (Gamma High Voltage Research). A syringe pump was used to feed the polymer solution into the needle tip and the feeding rate of syringe pump was fixed at 1.2 mL/h. An aluminum rotating disk (220 mm in diameter with a thickness of 10 mm) was located as the fiber collector at a fixed distance of 15 cm from the needle tip. Rotation speed of 500 rpm was used in this study. The polymer solution formed a Taylor cone at the tip of the needle by the combined force of gravity and electrostatic charge. A positively charged jet formed from the Taylor cone and sprayed to the grounded aluminum rotating disk, which collected the aligned nanofibers and kept their orientation. As-spun nanofibers were dried under vacuum at room temperature overnight. Morphology of the nanofiber mats was observed using a scanning electron microscope (SEM; JSM-5800LV, Jeol) (Fig. 1). The design parameters and performance indexes of scaffolds are shown in Table I.

Methods

Biotinylation of SCs. EZ-Link® Sulfo-NHS-Biotin (Pierce, Rockford, IL), a commercially available reagent, was applied to the biotinylating progress of SCs according to the operating manual. After being washed with the phosphate-buffered saline (PBS) at 37°C thrice, SCs adhering in a flask were treated with 2 mL of the biotinylating reagent (0.5 mM in PBS) in a CO_2 incubator for 30 min. Then the cells were washed with PBS at 37°C thrice, and immersed in iced PBS for 5 min. After shedding from the bottom of flask, the SCs were concentrated and resuspended to the desired concentration.

In order to identify the biotinylation of SCs, cells in the adhering and suspending state were fixed with 4% paraformaldehyde for 30 min, and so were the normal SCs (not biotinylated) as control. After being washed with PBS thrice,

TABLE I. The Design Parameters and Performance Indexes

Component	P(LLA-CL) (75:25)
Concentration (wt%)	8
Solvent	1,1,1,3,3,3-hexafluoro-2-propanol
Voltage (kV)	12
Flow rate (ml/h)	1.2
Collecting distance (cm)	15
MW (Da)	3.5×10^5
Fiber diameter (nm)	857.6
Thickness (μm)	100

cells were incubated with FITC-avidin (1:64 diluted in PBS; Boster, China) at room temperature for 5 min. After another three washes, cell nuclei were counterstained with the DAPI-staining solution (5 μg/mL in PBS; Beyotime, China) at room temperature for 20 min. After the final washes with PBS, the SCs were observed under a fluorescence microscope and the images were digitally recorded.

Avidin-treated scaffolds. Round 2D scaffolds of 7 mm in diameter were prepared and sterilized with ethanol (75%) overnight in a 96-well culture plate for all experiments. After three washes with PBS, the scaffolds were incubated with avidin (1 mg/mL in PBS; Sigma-Aldrich) at room temperature for 2 h. After other three washes with PBS, the scaffolds were prepared for use.

Cultivation of SCs. During the examination of attachment, proliferation, and morphology, two groups were designed, including the normal SCs on untreated scaffolds (the normal group) and the biotinylated SCs on avidin-treated scaffolds (the ABBS group).

In the detection of gene expressions, five groups were designed, including the normal SCs in the flask as control (the control group), normal SCs on untreated scaffolds (the normal group), normal SCs on avidin-treated scaffolds (the avidin group), the biotinylated SCs on avidin-treated scaffolds (the ABBS group), and the biotinylated SCs on untreated scaffolds (the biotin group).

In all groups, the SCs suspended in PBS with desired concentration were injected into each well. Then the culture wells were shaken at 100 rpm for 3 min and incubated at 37°C/5% CO_2 in a humidified environment. The complex of SCs and scaffolds was ready for further assays.

Attachment assay. As shown above, 2×10^4 cells suspended in PBS with a total volume of 20 μL were seeded onto scaffolds. In order to protect the growth and proliferation of cells, 200 μL of DMEM-F12 medium was injected into wells at 3 h after seeding. After incubation for 10 min, 30 min, 1 h, 3 h, 12 h, and 24 h, scaffolds were removed from the wells and washed with PBS gently to remove the nonattached cells. The cells on the scaffolds were then transferred onto a glass slide and fixed with 4% paraformaldehyde at room temperature for 30 min. After being washed for 3 times with PBS, cell nuclei were stained by the DAPI-staining solution (5 μg/mL in PBS) at room temperature for 20 min. After the final washes with PBS, the samples on glass slides were mounted with mounting fluid (50% glycerin in PBS) and covered with cover glass. All samples were observed with UV light using a fluorescence microscope. Six images (×400) randomly from either the middle or the border of each cultivation condition were taken and the stained cell nuclei in the images were counted. The number of cells in each display window was analyzed. Each experiment was performed six times in parallel.

Proliferation assay. SCs were seeded onto scaffolds with a density of 2×10^3 in PBS with a total volume of 20 μL and cultivated in 96-well culture plates up to 20 days. There were scaffolds in the blank wells without SCs as baseline. At regular two-day intervals (0, 2, 4, 6, 8, 10, 12, 14, 16, 18, and 20 days of cultivation after seeding), the proliferation of SCs was analyzed by Alamar blue assay, which is an established method for the fluorimetric measurement of cell growth as a function of mitochondrial activity in living cells.[19] Each experiment was performed six times in parallel. Two hundred microliters of fresh medium and 10 μL of Alamar blue dye were added to each well and incubated at 37°C/5% CO_2 for 4 h. Subsequently, 200 μL of the mixture of medium and Alamar blue dye was removed to the black wells and the fluorescence intensity (RFU) was detected with the exciting light of 545 nm and emitted light of 590 nm using a microplate reader (Bio-Rad, Munich, Germany).

Morphology

Immunostaining characterization. After cultivation for 4 and 14 days, respectively, the scaffolds were transferred onto the glass slides and fixed with 4% paraformaldehyde at room temperature for 30 min followed by washes for three times with PBS, and then blocked with 10% bovine serum albumin in PBS at room temperature for 30 min and washed again with PBS. Scaffolds were then incubated with rabbit anti-S100 (polyclonal; 1:100 diluted in PBS; Boster, China) at 4°C overnight. Scaffolds without primary antibody incubation served as a blank control. After another three washes with PBS, the scaffolds were further incubated with Cy3-goat anti-rabbit IgG (Beyotime, China) at room temperature for 2 h. Cell nuclei were counterstained with DAPI (5 μg/mL in PBS) at room temperature for 20 min. After the final washes with PBS, the scaffolds on glass slides were mounted with mounting fluid and covered with cover glass. Labeled samples were visualized under a laser scanning confocal fluorescence microscope (LSCM) and the images were digitally recorded.

Scanning electron microscopy. After cultivation for 14 days, the samples were removed from the wells and fixed with 2.5% glutaraldehyde solution at 4°C overnight. Subsequently, the samples were postfixed with 1% OsO_4, dehydrated in graded acetone, and dried with a critical point drier (Hitachi, Tokyo, Japan). After this, the samples were coated with gold in a JFC-1100 unit (Jeol Inc., Japan) and observed under a SEM (JEM-T300, Jeol Inc., Japan). The images were digitally recorded.

Detection of gene expressions. In order to investigate the effect of ABBS on SCs gene expressions clearly, five groups were designed as shown above, including the control group, the normal group, the avidin group, the ABBS group, and the biotin group. The expressions of S100, brain derived neurotrophic factor (BDNF), glia derived neurotrophic factor (GDNF), nerve growth factor (NGF), ciliary neurotrophic factor (CNTF), and peripheral myelin protein 22 (PMP22) were detected by the real-time reverse transcription polymerase chain reaction (real-time PCR).

TABLE II. The Designed Primers of Seven Genes for Real-Time PCR

Gene	Primer sequence	Gene bank	Length
β-Actin	F:5′-CACCCGCGAGTACAACCTTC-3′ R:5′-CCCTATCCCACCATCACACC-3′	NM_031144	207
S100b	F:5′-GGGTGACAAGCACAAGCTGAA-3′ R:5′-AGCGTCTCCATCACTTTGTCCA-3′	NM_013191	117
GDNF	F:5′-GGCGACGGGACTCTAGAATGA-3′ R:5′-GTCAGGATAATCTTCGGGCATATTG-3′	NM_019139	194
BDNF	F:5′-TCCTGATAGTTCTGTCCATTCAGCA-3′ R:5′-GCCATTCATTCAGGCTTCCA-3	NM_012531	93
NGF	F:5′-TGATCGGCGTACAGGCAGA-3′ R:5′-GAGGGCTGTGTCAAGGGAAT-3′	XM_227525	107
CNTF	F:5′-TTTGCGAGAGCAAACACCTCT-3′ R:5′-TGCTAGCCAGATAGAACGGCTAC-3′	NM_013166	67
PMP22	F:5′-TGTACCACATCCGCCTTGG-3′ R:5′-GAGCTGGCAGAAGAACAGGAAC-3′	NM_017037	138

After cultivation for 14 days, total RNA was extracted from the SCs in all groups by homogenizing in TRIzol reagent (Invitrogen, Carisbad, USA). RT-PCR analysis was performed at 37°C for 15 min, followed by 85°C for 15 s in 20 μL of reaction mixture (as described by TAKARA, Japan) with Ready-To-Go You-Prime First-Strand Beads (Bio Rad, USA). Real-time PCR was performed using the Light Cycler rapid thermal cycler system (Bio Rad, IQ5, USA). Amplification reactions were performed in 25 μL of reaction mixture (TAKARA, Japan). The amplification protocol consisted of one cycle at 95°C for 10 s followed by 40 cycles at 95°C for 5 s, 60°C for 20 s, and 72°C for 30 s. Detection of the fluorescent products was carried out at the end of the 72°C extension period.

The gene of β-actin was performed as the internal control. The following forward (F) and reverse (R) primers of all genes (Sangon, Shanghai) were designed and applied in the present study (Table II).

Statistical analysis

All data were first adjusted by the square root transformation using Student's *t* test or Mann-Whitney U-test. If data were normally distributed and the variances between all groups were homogeneous prior to analysis, they would be presented as the mean values ± standard deviation of six replicates for each sample using Student's two tailed *t* test; or they would be analyzed using Mann-Whitney U-test. Particularly, the relative quantitative method of (1+E)-ΔΔCt was applied in the analysis of real-time PCR.[20]

RESULTS

Identification of biotinylated SCs

After being incubated with avidin-FITC, all biotinylated SCs on the bottom of the flask showed a green appearance around the cell membrane under the fluorescence microscope [Fig. 2(a)], while the normal cells that were not biotinylated did not show any green fluorescence (images not shown). Figure 2(b) further demonstrated that when the biotinylated SCs detached from the bottom of flask and

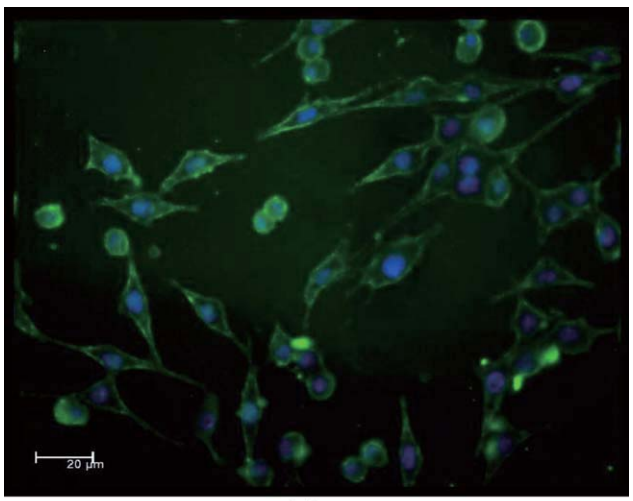

FIGURE 2. Fluorescent micrographs of biotinylated SCs attaching onto the bottom of the flask (a) and suspending in PBS (b). [Color figure can be viewed in the online issue, which is available at wileyonlinelibrary.com.]

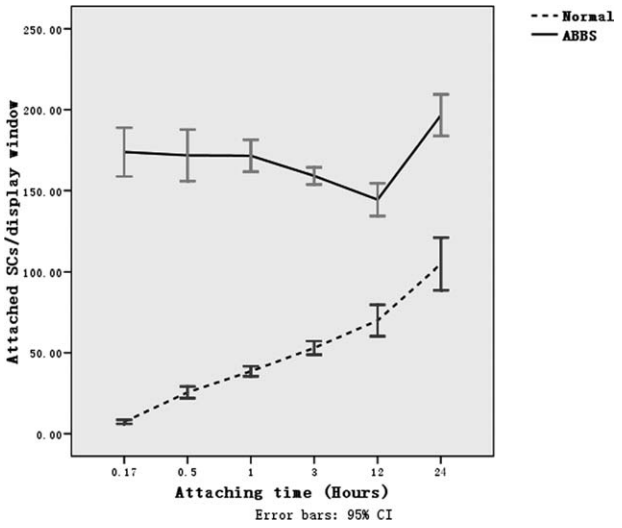

FIGURE 3. The mean number of attached SCs in per display window from the normal group (the normal SCs on untreated scaffolds) (- - -) and the ABBS group (the biotinylated SCs on avidin-treated scaffolds)(—) after attaching for 10 min, 30 min, 1 h, 3 h, 12 h, and 24 h, respectively.

suspended in PBS, the FITC-avidin still attached onto the membrane of SCs, which meant that the molecules of biotin kept around SCs.

Attachment assay

The curves in Figure 3 indicated that the number of SCs in the ABBS group were much higher than that of SCs in the normal group within 24 h. Especially at 10 min, the attached biotinylated SCs were about 24 times more than the attached normal SCs (173.81 $\pm$ 14.35 vs. 7.33 $\pm$ 1.20; $p < 0.05$). The number of attached SCs in the ABBS group decreased with the attaching time and downed to the least at 12 h, which was still higher than that in the normal group (144.36 $\pm$ 9.65 vs. 69.95 $\pm$ 9.24; $p < 0.05$). But after 12 h, the number of attached SCs in the ABBS group began to increase and reached a peak value at 24 h, which was even higher than that at 10 min.

Proliferation assay

Figure 4 showed the proliferation of SCs on scaffolds in the normal groups and ABBS group. The curves indicated that the proliferating tendency of SCs in the normal group kept increasing within 14 days. On the other hand, the proliferation of SCs in the ABBS group decreased in the first 2 days and even did not return to the initial level at 4 days. But after 4 days, it began to increase and kept increasing at high speed until 14 days. The peak value of the proliferation of SCs in the ABBS group was a little higher than that of SCs in the normal group ($p < 0.05$).

Morphology of SCs

After cultivation for 4 days, the morphology of SCs between the two groups was greatly different. Most of the SCs in the normal group showed the typical spindle-shape [Fig. 5(a)], while most of SCs in the ABBS group kept the spherical shape still and did not proliferate [Fig. 5(b)]. But after cultivation for 14 days, there were no great significant differences of the SCs' morphology between the two groups, which all showed a mature bipolar shape. Additionally, fluorescent micrographs showed the alignment of SCs clearly. The scanning micrographs of Figure 6(a,b) further proved that the orientation of SCs was along with the alignment of nanofibers. Furthermore, Figure 6(a,b) showed that the ECM secreted by SCs spread around the cell membrane and upon the surface of scaffolds. The autogenous ECM combined SCs together, forming a membrane on the surface of the scaffolds.

Detection of gene expressions

The gene expressions of S100, GDNF, BDNF, NGF, CNTF, and PMP22 are displayed in Figures 7 and 8. Compared with the gene expressions of SCs in the control group, those of SCs in the normal group were down-regulated slightly ($p < 0.05$) except the gene of S100, while those of SCs in the avidin group were maintained mostly except those of BDNF and NGF which were down-regulated ($p < 0.05$). On the other hand, all gene expressions of SCs in both the ABBS group and biotin group were greatly up-regulated significantly ($p < 0.05$). In particular, the S100 gene expression of biotinylated SCs was up-regulated more greatly. In addition, the up-regulation of S100, BDNF, and NGF gene expressions of SCs in the biotin group was even higher than that of SCs in the ABBS group.

DISCUSSION

Effective SCs attaching onto scaffolds steadily is a critical step for the fabrication of tissue-engineered nerve. Recently, ABBS was found to be a powerful tool that enhanced cell attaching onto synthetic scaffolds in tissue engineering. The interaction between avidin and biotin is the strongest

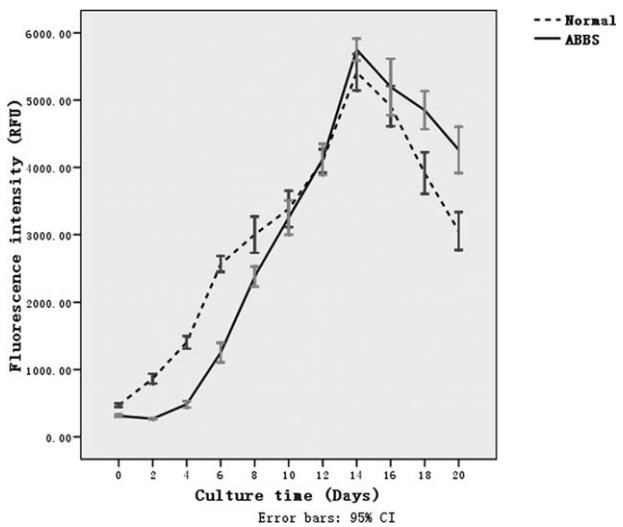

FIGURE 4. Proliferation curve for SCs. The SCs proliferation in the normal group (the normal SCs on untreated scaffolds) (- - -) and the ABBS group (the biotinylated SCs on avidin-treated scaffolds) (—) was detected after cultivation for (0), 2, 4, 6, 8, 10, 12, 14, 16, 18, and 20 days, respectively.

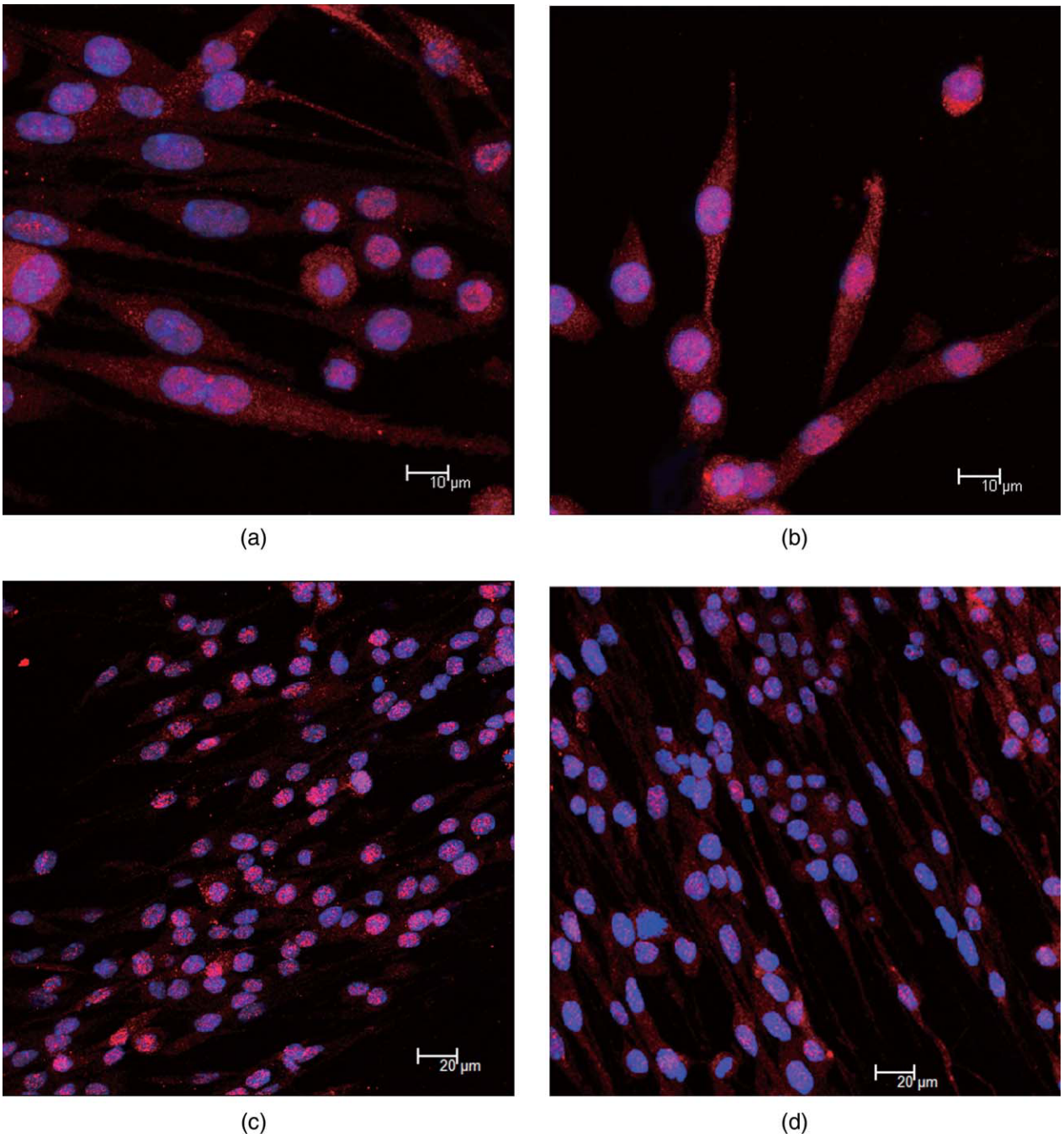

FIGURE 5. LSCM fluorescent micrographs of SCs. (a) and (c) are micrographs for SCs in the normal group (the normal SCs proliferating on untreated scaffolds) after cultivation for 4 and 14 days, respectively. (b) and (d) are micrographs for SCs in the ABBS group (the biotinylated SCs proliferating on avidin-treated scaffolds) after cultivation for 4 and 14 days, respectively. [Color figure can be viewed in the online issue, which is available at wileyonlinelibrary.com.]

known noncovalent biochemical bond that provides a mechanism for the quick and stable attachment of cells onto scaffolds.[21] With this advantage, ABBS has been used in hepatic tissue engineering and cartilage tissue engineering in *in vitro* tests.[15,16] However, the effect of ABBS on the SCs attaching onto the electrospun scaffolds has not been determined.

In former studies, ABBS was suggested to promote the attaching of cells onto the surface of scaffolds obviously even within a very short time, which was also proved in the present study. Within 10 min, the biotinylated SCs attached onto avidin-treated scaffolds more rapidly than the normal SCs attaching onto untreated scaffolds, and the difference of cells number/display window between the two groups was

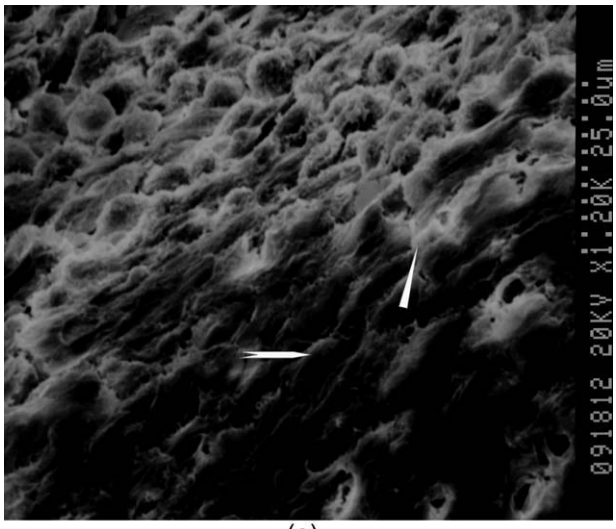

FIGURE 6. SEM scanning micrographs of SCs in the normal group (the normal SCs proliferating on untreated scaffolds) (a) and SCs in the ABBS group (the biotinylated SCs proliferating on avidin-treated scaffolds) (b) after cultivation for 14 days. The micrographs showed the SCs (⇨), ECM (▷), and nanofibers (⇨) clearly.

significant ($p < 0.05$). This result conformed to the finding of Kojima et al., which suggested that momentary contact might be sufficient to stably trap hepatic cells on surfaces when ABBS was used.[16] But we further found that the number of attached biotinylated SCs in the ABBS group began to decrease slightly after 4 h, and downed to the least at 12 h, but was still apparently higher than that of the attached normal SCs in the normal group ($p < 0.05$). This finding was similar to what Tsai et al. found,[15] which might be due to the internalization of membrane-conjugated biotin molecules. It has been reported that fluorescence-labeled avidin binding throughout biotinylated cells shifted to the cell interior at 24 h.[22] Therefore, biotinylated cells attaching onto avidin-treated scaffolds might detach because of the loss of biotin. But the number of attached biotinylated SCs begun

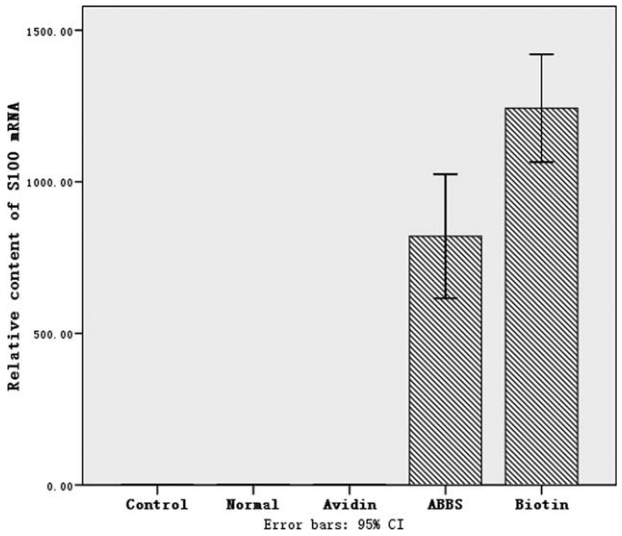

FIGURE 7. The real-time PCR analysis of S100 of the normal SCs on untreated scaffolds (the normal group), the normal SCs on avidin-treated scaffolds (the avidin group), the biotinylated SCs on avidin-treated scaffolds (the ABBS group), and the biotinylated SCs on untreated scaffolds (the biotin group) after cultivation for 14 days, with the gene expressions of the normal SCs in the flask as control (the control group).

to pick up and kept increasing from 12 to 24 h, which indicated that there were other factors contributing to the SCs' attachment. We supposed that the ECM secreted by SCs might play a role. The ECM bonds complemented the binding strength after the loss of ABBS. The autogenous ECM could combine ordered SCs of single layer together and form a membrane upon the surface of the scaffolds [Fig. 6(b)]. Kojima et al. also considered that the hepatic cells

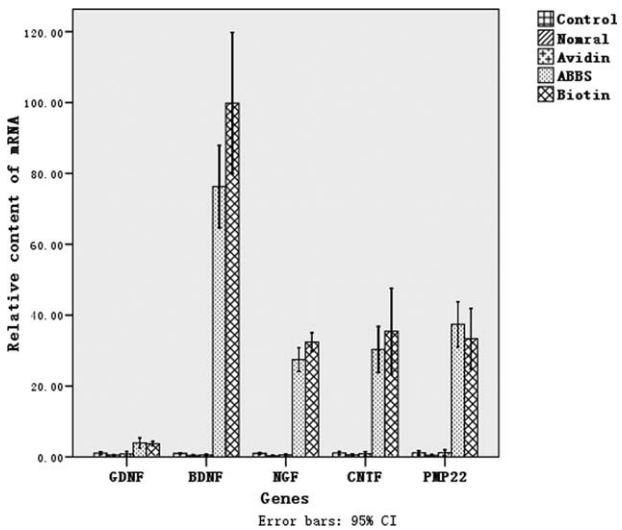

FIGURE 8. The real-time PCR analysis of GDNF, BDNF, NGF, CNTF, and PMP22 expressions of the normal SCs on untreated scaffolds (the normal group), the normal SCs on avidin-treated scaffolds (the avidin group), the biotinylated SCs on avidin-treated scaffolds (the ABBS group), and the biotinylated SCs on untreated scaffolds (the biotin group) after cultivation for 14 days, with the gene expressions of the normal SCs in the flask as control (the control group).

trapped with ABBS on an avidin-absorbed surface could finally spread using their own adherent molecules, such as integrin.[16] These analyses indicated that the role of ABBS might provide high affinity binding that stabilized cell membrane attachment onto the surface and enabled increased binding of ECM to the surface of scaffolds, thus increasing the membrane/substrate contact area.[23] The high affinity binding provided by ABBS was necessary and critical for the promotion of SCs attachment with lack of ECM in early time.

Enhancement of cell attaching onto synthetic scaffolds was an initial step for applying ABBS to tissue engineering. The next step was to ensure that attached biotinylated SCs could proliferate and perform their normal functions. In the study of Prichard et al., the biotinylated adult adipose-derived stem cells (ASCs) were seeded onto avidin/fibronectin-treated biomaterials, and at last no significant differences in proliferation, metabolism, intracellular ATP, or intracellular caspase-3 activity were observed.[24] In the present study, the proliferation assay showed that the fluorescence intensity of the ABBS group decreased in the first 2 days and downed to the least at 4 days, which meant that the rate of the metabolism and proliferation of biotinylated SCs on avidin-treated scaffolds decreased. So the SCs' morphology was investigated after cultivation for 4 days. The micrographs indicated that compared with the morphology of SCs in the ABBS group, that of SCs in the normal group was more mature and atypical, which was another evidence of the temporary effect of ABBS on SCs' proliferation [Fig. 5(a,b)]. Tsai et al. assumed that the temporary decrease of the proliferation of biotinylated cells might be due to the internalization of membrane-conjugated biotin molecules.[15] Nevertheless, biotinylated SCs began to proliferate at higher speed with the culturing time than the normal SCs afterward. After cultivation for 14 days, SCs not only in the normal group but also in the ABBS group proliferated remarkably (Fig. 4), and there were no significant differences of SCs' morphology between the two groups [Figs. 5(c,d) and 6(a,b)]. The possible reason might be that the surface-bound avidin was replaced by autogenous ECM which was very suitable for SCs' growth. This result eliminated the adverse effect of ABBS on the proliferation of SCs in the long term.

Another crucial issue regarding the application of ABBS to neural tissue engineering was whether ABBS altered the SCs' phenotype. After cultivation for 14 days, when the proliferation of SCs reached its peak, the expressions of six important genes, including S100, GDNF, BDNF, NGF, CNTF, and PMP22, were detected by real-time PCR. S100, as the special marker of SCs, was known to be released into the extracellular space to stimulate neuronal survival, proliferation, and differentiation.[25] Furthermore, the presence of S100 has been found to be related to the nutrition of SCs and considered as a sign of SCs' maturation.[26] GDNF, BDNF, NGF, and CNTF, as the most familiar four kinds of neurotrophin so far, were considered to nourish different kinds of neurons.[27] Brandt et al. proved that the acutely dissociated SCs used in tendon autografts promoted axonal outgrowth more greatly than untreated SCs in peripheral nerve defects, which was attributed to the up-regulation of neurotrophin.[28] Previous studies proved the promotion of the regeneration of axons by complementing exogenous neurotrophin or up-regulating neurotrophic gene expression.[29–32] PMP22, as the primary component of myelin protein, was known to be involved in controlling myelin thickness and stability. It played an important role in the formation of myelin sheath.[33] D'Urso reported that the overexpressing or underexpressing PMP22 did not affect the myelination greatly in *vitro* test.[34] But Magyar et al. found that the transgenic mice that carried additional copies displayed a severe congenital hypomyelinating neuropathy as characterized by an almost complete lack of myelin and marked slowing of nerve conductions.[35] In the present study, the comparison of the five groups obviously indicated that all gene expressions of SCs in the normal group were down-regulated slightly except the S100 gene, which conformed to the result of Chew et al.[36] But all gene expressions of SCs in the avidin group were maintained except those of BDNF and NGF which were down-regulated slightly (Fig. 7). These analyses showed that the avidin-treated scaffolds could provide a more favored environment for SCs than the untreated scaffolds. On the other hand, all gene expressions of SCs in both the ABBS group and the biotin group were up-regulated significantly ($p < 0.05$) (Figs. 7 and 8). It was clear from the foregoing that the up-regulation of gene expressions was induced by biotin rather than aligned scaffolds or avidin-treated scaffolds. According to the report of Tsai et al.,[15] the membrane-conjugated biotin molecules might be internalized into the plasma or nuclei of SCs, thus regulating gene expressions. Additionally, that the up-regulation of the gene expressions of SCs in the biotin group was even higher than that of SCs in the ABBS group indicated that avidin weakened the effect of biotin on SCs' gene expressions. One of the reasons might be that the stable binding between avidin and biotin could prevent the internalization of membrane-conjugated biotin molecules. These hypotheses need to be proved in the ongoing study. Nevertheless, the significant up-regulation of S100 mRNA might indicate further differentiation and maturation of SCs, which could benefit axonal regeneration. In addition, the obvious up-regulation of neurotrophin gene expressions resulting from the stimulation of ABBS would provide a more favorable microenvironment for the repair of the peripheral nerve. But the result of up-regulation of the PMP22 gene is still not clear, and its effect on myelination needs further investigation in *in vivo* tests.

CONCLUSIONS

The present study first demonstrated that ABBS could help SCs attach onto the surface of scaffolds effectively within a short time, providing a feasible approach toward the fabrication of tissue-engineered nerve. Meanwhile, ABBS enhanced SCs to mature and synthesize more neurotrophin without adverse effects in the long term, fabricating a more favorable microenvironment for the repair of the peripheral nerve. The current study provided an insight into the application of ABBS in promoting neural tissue engineering.

REFERENCES

1. Silvia P, Carla C, Joseph L, Ubaldo DC, Francesca T, Stefano A, Angelo V, Fabrizio G. Electrospun micro- and nano-fiber tubes for functional nervous regeneration in sciatic nerve transections. BMC Biotechnol 2008;8:39.
2. Koh HS, Yong T, Chan CK, Ramakrishna S. Enhancement of neurite outgrowth using nano-structured scaffolds coupled with laminin. Biomaterials 2008;29:3574–3582.
3. Meek MF, Coert JH. US Food and Drug Administration/Conformit Europe-approved absorbable nerve conduits for clinical repair of peripheral and cranial nerves. Ann Plast Surg 2008;60:466–472.
4. Willerth SM, Sakiyama-Elbert SE. Approaches to neural tissue engineering using scaffolds for drug delivery. Adv Drug Deliv Rev 2007;59:325–338.
5. Bruns S, Stark Y, Wieland M, Stahl F, Kasper C, Scheper T. Fast and efficient screening system for new biomaterials in tissue engineering: A model for peripheral nerve regeneration. J Biomed Mater Res A 2007;81:736–747.
6. Tsai WB, Wang PY, Chang Y, Wang MC. Fibronectin and culture temperature modulate the efficacy of an avidin-biotin binding system for chondrocyte adhesion and growth on biodegradable polymers. Biotechnol Bioeng 2007;98:498–507.
7. Armstrong SJ, Wiberg M, Terenghi G, Kingham PJ. ECM molecules mediate both Schwann cell proliferation and activation to enhance neurite outgrowth. Tissue Eng 2007;13:2863–2870.
8. Balcells M, Edelman ER. Effect of pre-adsorbed proteins on attachment, proliferation, and function of endothelial cells. Cell Physiol 2002;191(2):155–161.
9. Schmidt CE, Leach JB. Neural tissue engineering: Strategies for repair and regeneration. Annu Rev Biomed Eng 2003;5:293–347.
10. Bini TB, Gao S, Wang S, Ramakrishna S. Development of fibrous biodegradable polymer conduits for guided nerve regeneration. Mater Sci Mater Med 2005;16:367–375.
11. Kuramitz H, Sugawara K, Tanaka S. Electrochemical sensing of avidin-biotin interaction using redox markers. Electroanalysis 2000;20:1299–1303.
12. Green N. Avidin. Adv Prot Chem 1975;29:85–133.
13. Akiyama SK, Yamada KM. The interaction of plasma fibronectin with fibroblastic cells in suspension. Biol Chem 1985;60:4492–4500.
14. Kuo SC, Lauffenburger DA. Relationship between receptor/ligand binding affinity and adhesion strength. Biophysics 1993;65: 2191–2200.
15. Tsai WB, Wang MC. Effect of an avidin-biotin binding system on chondrocyte adhesion, growth and gene expression. Biomaterials 2005;26:3141–3151.
16. Kojima N, Matsuo T, Sakai Y. Rapid hepatic cell attachment onto biodegradable polymer surfaces without toxicity using an avidin-biotin binding system. Biomaterials 2006;27:4904–4910.
17. Bhat VD, Truskey GA, Reichert WM. Fibronectin and avidin-biotin as a heterogeneous ligand system for enhanced endothelial cell adhesion. J Biomed Mater Res 1998;41:377–385.
18. Mo XM, Xu CY, Kotaki M, Ramakrishna S. Electrospun P(LLA-CL) nanofiber: A biomimetic extracellular matrix for smooth muscle cell and endothelial cell proliferation. Biomaterials 2004;25:1883–1890.
19. Page B, Page M. Sensitive colorimetric cytotoxicity measurement using alamar blue. Oncol Rep 1995;2:59–61.
20. Liu WH, Saint DA. A new quantitative method of real time reverse transcription polymerase chain reaction assay based on simulation of polymerase chain reaction kinetics. Anal Biochem 2002; 302:52–59.
21. Wojda U, Goldsmith P, Miller JL. Surface membrane biotinylation efficiently mediates the endocytosis of avidin bioconjugates into nucleated cells. Bioconjug Chem 1999;10:1044–1050.
22. Bayer EA, Wilchek M. The use of the avidin-biotin complex as a tool in molecular biology. Meth Biochem Anal 1980;26:1–45.
23. Chan BP, Bhat VD, Yegnasubramanian S, Reichert WM, Truskey GA. An equilibrium model of endothelial cell adhesion via integrin-dependent and integrin-independent ligands. Biomaterials 1999;20:2395–2403.
24. Prichard HL, Reichert WM, Klitzman B. Adult adipose-derived stem cell attachment to biomaterials. Biomaterials 2007;28: 936–946.
25. Huang YL, Ding M, Hansson HA. Dorsal root ganglion nerve cells transiently express increased immunoreactivity of the calcium-binding protein S-100b after sciatic transection. Brain Res 1998; 785:351–354.
26. Lin WW, Chen X, Wang XD, Liu J, Gu XS. Adult rat bone marrow stromal cells differentiate into Schwann cell-like cells in vitro. Animal 2008;44:31–40.
27. Terenghi G. Peripheral nerve regeneration and neurotrophic factors. J Anat 1999;194:1–14.
28. Brandt J, Nilsson A, Kanje M, Lundborg G, Dahlin LB. Acutely dissociated Schwann cells used in tendon autografts for bridging nerve defects in rats: A new principle for tissue engineering in nerve reconstruction. Scand J Plast Reconstr Surg Hand Surg 2005;39:321–325.
29. Sendtner M, Schmalbruch H, Stöckli KA, Carroll P, Kreutzberg GW, Thoenen H. Ciliary neurotrophic factor prevents degeneration of motor neurons in mouse mutant progressive motor neuropathy. Nature 1992;358:502–504.
30. Yu XJ, Bellamkonda RV. Tissue-engineered scaffolds are effective alternatives to autografts for bridging peripheral nerve gaps. Tissue Eng 2003;9:421–430.
31. Fine EG, Decosterd I, Papaloizos M, Zurn AD, Aebischer P. GDNF and NGF released by synthetic guidance channels support sciatic nerve regeneration across a long gap. Eur J Neurosci 2002;15:589–601.
32. Haastert K, Grothe C. Gene therapy in peripheral nerve reconstruction approaches. Curr Gene Ther 2007;7:221–228.
33. Adlkofer K, Frei R, Neugerg DH-H, Zielasek J, Toyka KV, Suter U. Heterozygous peripheral myelin protein 22-deficient mice are affected by a progressive demyelinating tomaculous neuropathy. Neuroscience 1997;17:4662–4671.
34. D'Urso D, Schmalenbach C, Zoidl Georg, Prior R, Muller HW. Studies on the effects of altered PMP22 expression during myelination in vitro. Neurosci Res 1997;48:31–42.
35. Magyar JP, Martini R, Ruelicke T, Aguzzi A, Adlkofer K, Dembic Z, Zielasek J, Toyka KV, Suter U. Impaired differentiation of Schwann cells in transgenic mice with increased PMP22 gene dosage. Neuroscience 1996;16:5351–5360.
36. Chew SY, Mi R, Hoke A, Leong KW. The effect of the alignment of electrospun fibrous scaffolds on Schwann cell maturation. Biomaterials 2008;29:653–661.